Widespread Ground Motion Distribution Caused by Rupture Directivity during the 2015 Gorkha, Nepal Earthquake

Kazuki Koketsu[1], Hiroe Miyake[2] , Srinagesh Davuluri[3] and Soma Nath Sapkota[4]

1. Corresponding Author. Professor, Earthquake Research Institute, University of Tokyo, Tokyo 113-0032, Japan. Email: koketsu@eri.u-tokyo.ac.jp

2. Associate Professor, Earthquake Research Institute, University of Tokyo, Tokyo 113-0032, Japan. Email: hiroe@eri.u-tokyo.ac.jp

3. Chief Scientist, National Geophysical Research Institute, Hyderabad, India. Email: srinagesh@ngri.res.in

4. Deputy Director General, Department of Mines and Geology, Kathmandu, Nepal. Email: somanathsapkota@yahoo.com

Abstract

The ground motion and damage caused by the 2015 Gorkha, Nepal earthquake can be characterized by their widespread distributions to the east. Evidence from strong ground motions, regional acceleration duration, and teleseismic waveforms indicate that rupture directivity contributed significantly to these distributions. This phenomenon has been thought to occur only if a strike-slip or dip-slip rupture propagates to a site in the along-strike or updip direction, respectively. However, even though the earthquake was a dip-slip faulting event and its source fault strike was nearly eastward, evidence for rupture directivity is found in the eastward direction. Here, we explore the reasons for this apparent inconsistency by performing a joint source inversion of seismic and geodetic datasets, and conducting ground motion simulations. The results indicate that the earthquake occurred on the underthrusting Indian lithosphere, with a low dip angle, and that the fault rupture propagated in the along-strike direction at a velocity just slightly below the S-wave velocity. This low dip angle and fast rupture velocity produced rupture directivity in the along-strike direction, which caused widespread ground motion distribution and significant damage extending far eastwards, from central Nepal to Mount Everest.

Keywords: seismic ground motion, rupture directivity, low-angle dip slip

INTRODUCTION

The Gorkha earthquake occurred on 25 April 2015 (UT) in the north part of central Nepal, causing widespread damage with more than 8,000 fatalities. In the Himalayan region, including Nepal, the Indian plate is colliding with the southern margin of the Eurasian plate, and the Indian lithosphere underthrusts beneath the Himalayas along the Main Himalayan Thrust (MHT), which reaches the ground surface at the Main Frontal Thrust (MFT; Fig. 1a). This underthrusting generates large Himalayan earthquakes, the hazards of which have been noted for decades, together with the seismic vulnerability of the countries around the Himalayas. According to the tectonics described above and the result of the Global CMT Project (GCMT), the focal mechanism of the Gorkha earthquake was dip-slip rupture with a strike of west-northwest (WNW).

Rupture directivity is a combined effect of rupture propagation, the earthquake source radiation pattern, and particle motion polarization on seismic ground motions. This effect is known to cause directional variations in seismic ground motion and damage, and to occur if a strike-slip or dip-slip rupture propagates to a site in the along-strike or updip direction, respectively. However, although the focal mechanism of the 2015 Gorkha earthquake was dip-slip faulting, as mentioned above, rupture directivity was found in the Kathmandu Valley, which is located in the nearly along-strike direction.
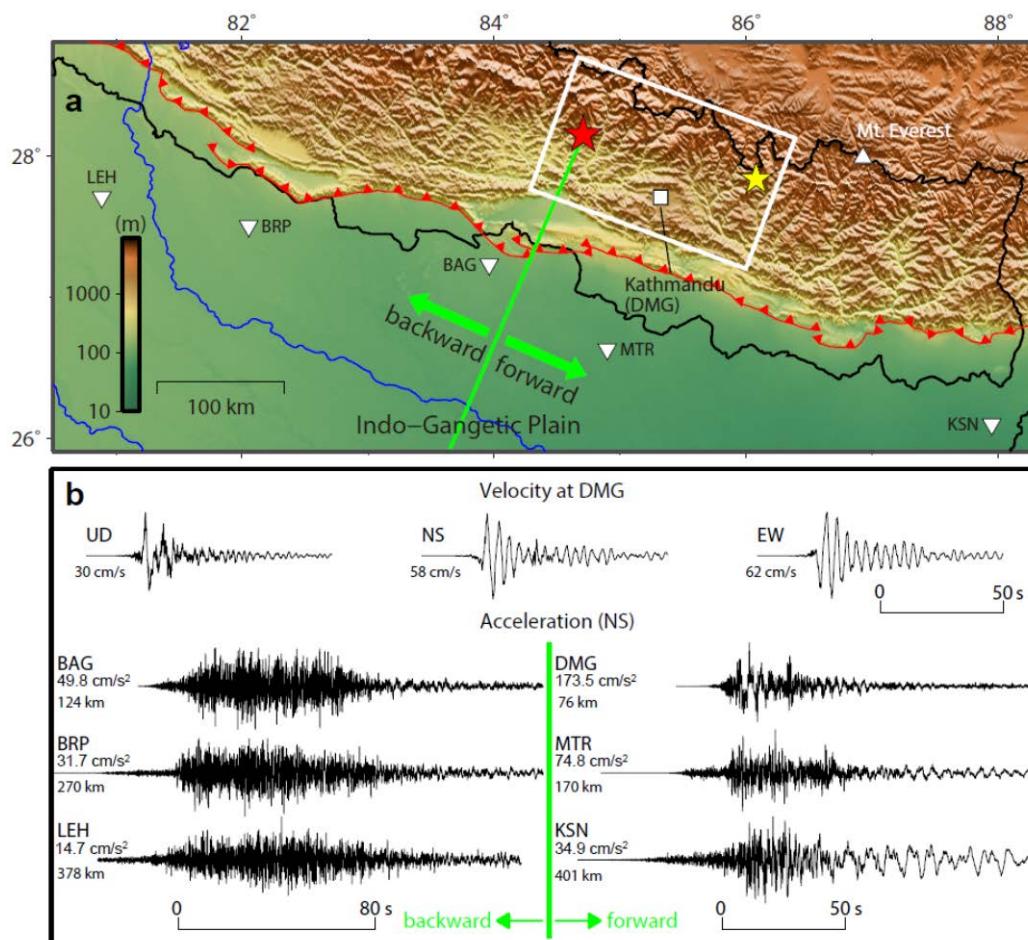
Figure 1. Index map and seismograms in Nepal and India for Gorkha earthquake.

The ground motions observed by the Department of Mines and Geology (DMG) of Nepal in Kathmandu during the earthquake (upper traces in Fig. 1b) show large pulse-like waveforms, especially in the vertical component, although the later parts of

the horizontal components were complicated by the basin effects of the Kathmandu Valley. Such ground motion pulses are considered to be firm evidence of rupture directivity. The occurrence of rupture directivity was also confirmed by the regional acceleration seismograms in the lower traces in Fig. 1b, where the strong-motion duration in the forward direction is shorter than in the backward direction. The teleseismic displacement seismograms show both the large pulse-like waveforms and shorter ground motion duration in the forward direction.

Here, we first explore the reasons why along-strike rupture directivity occurred during the dip-slip Gorkha earthquake, by performing a joint source inversion of waveform and geodetic datasets. We next examine the relationship between enhanced ground motion amplitudes and rupture directivity by conducting ground motion simulations. It is noted that this paper is a concise version of Koketsu *et al.* (2016).

RESULTS

In order to explore the reasons underlying the apparent inconsistency mentioned above, it is crucial to investigate the rupture process of the Gorkha earthquake. First, we constructed the source fault model of strike = 290° and dip = 7° (Fig. 1a), using the distribution of the main shock and aftershocks, and the quick GCMT solution. It is noted here that the dip angle of the source fault is as low as 7°. We then carried out a joint inversion of waveform and geodetic datasets. Two types of waveform datasets were available for this inversion: 1) the global seismograms which were obtained from the Global Seismographic Network through the Data Management Center of the Incorporated Research Institutions for Seismology, and 2) the local seismograms which were observed at strong motion stations and high-rate GPS stations. Two types of geodetic datasets were also available for this inversion: 1) horizontal and vertical ground deformations at static GPS stations, and 2) line-of-sight ground deformations shown in Supplementary Fig. 2c, which were derived from the processed InSAR image.

The resultant total slip distribution from the inversion is shown in Fig. 2a, with a maximum value of 6.4 m. The calculated seismic moment was 8.6×10^{20} Nm, which yielded an M_w of 7.9. The Most of the synthetics show good fit, but those for the horizontal components of local seismograms underestimate the observations because of the limitations of the 1-D velocity structure constructed. Snapshots of the slip distribution were taken every 10 s after the rupture initiation at the hypocentre (Fig. 2b), showing that the rupture propagated eastward nearly along the strike, at an almost constant velocity of about 3.3 km/s, which is slightly lower than the *S*-wave velocity of 3.5 km/s on the source fault.
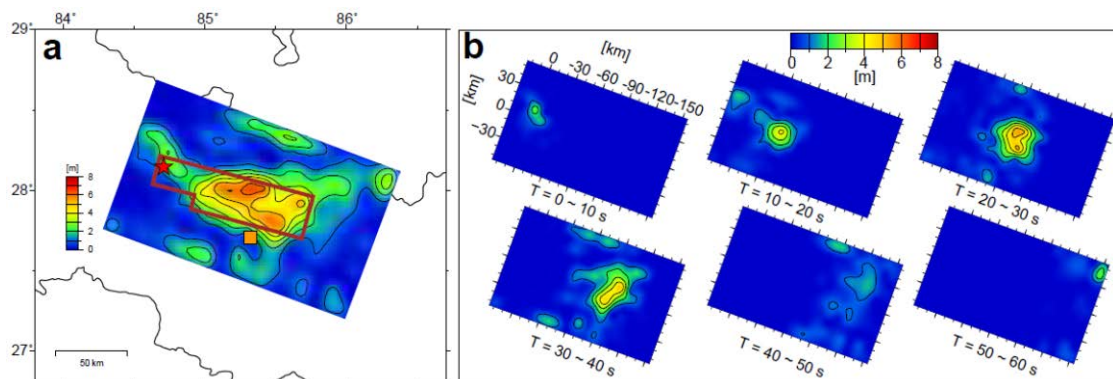
Figure 2. Results of the source inversion.

As for a strike-slip earthquake such as the 1995 Kobe earthquake, in this case

along-strike rupture propagation caused the directivity effects, producing constructive interference of seismic waves in the forward direction. *S*-waves from the fault segments arrived almost simultaneously along the rupture direction. They resulted in the pulse-like shape and long-period feature of the strong motion seismograms such as those observed in the Kathmandu Valley (Figs. 1b), and a zone of large ground motion spreading beyond the main rupture area. The latter feature cannot be generated by factors other than rupture directivity.

However, for dip-slip earthquakes, rupture directivity has not been thought to occur during along-strike rupture propagation, such as in the Gorkha earthquake. Actually, if the rupture velocity is close to the S-wave velocity and the faulting mechanism is nearly uniform, constructive interference of seismic waves or a ground motion pulse can occur in any rupture direction, but a 'large' ground motion pulse has to occur for the identification of rupture directivity. This condition can be satisfied if large ground motions are generated along the rupture direction. For a typical dip slip with a dip angle of 45°, large ground motions are generated only along the updip direction because of its *S*-wave radiation pattern, and therefore, the rupture directivity is visible only during the updip rupture propagation of a typical dip-slip earthquake.

In contrast, the rupture directivity cannot be seen during along-strike rupture propagation of a typical dip-slip earthquake, because the nodal plane of the S-wave radiation pattern extends in the along-strike direction. However, if the dip angle is as low as that of the Gorkha earthquake, the ground above the dip slip is located in a lobe of the radiation pattern, and the rupture directivity occurs during along-strike rupture propagation (Fig. 3). The strong motion seismograms observed in the Kathmandu Valley and regional and teleseismic waveforms (Figs. 1b) provide, for the first time, conclusive evidence of rupture directivity during the along-strike rupture propagation of a low-angle dip-slip earthquake.
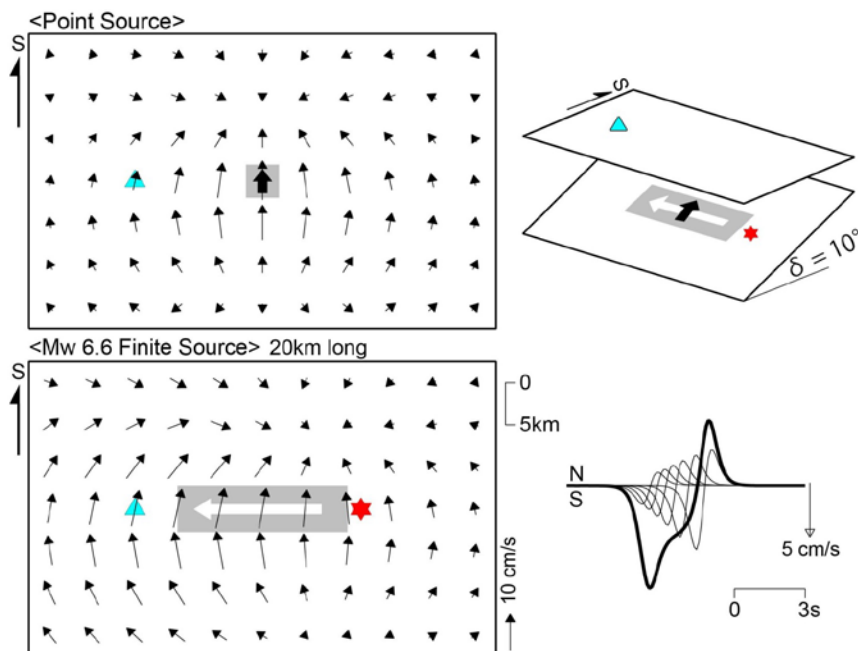
Figure 3. Schematic illustration of rupture directivity for a low-angle dip-slip earthquake (10° dip).

In Martin et al. (2015), nearly 4,000 macroseismic effects of the Gorkha earthquake had been collected, and converted into shaking intensities through detailed assessments. The distribution of resultant intensities in Fig. 4a shows that intensities of 7 or larger are mostly concentrated in a 100 km wide zone extending east-southeast from the main shock epicentre. However, since no intensity was obtained between the

longitudes of 86 and 87°E along the extension, we cannot determine the eastern end of the high intensity zone.

To compensate for these missing data, we calculated the distribution of the fatality rate, which is the ratio of the number of fatalities to the total population in a district. According to this distribution, we found districts between 86 and 87°E to have fatality rates of 0.01 to 0.1%, which correspond to an intensity of 7. In these far eastern districts, included is the district of Mount Everest, where avalanches induced by seismic ground motions killed 20 people and injured 120 people. Therefore, it has been realized that the high intensity zone was extended from the main shock epicentre in central Nepal to Mount Everest. Enhanced shaking due to along-strike rupture directivity of the Gorkha earthquake likely played an important contributing role to this widespread ground motion distribution.
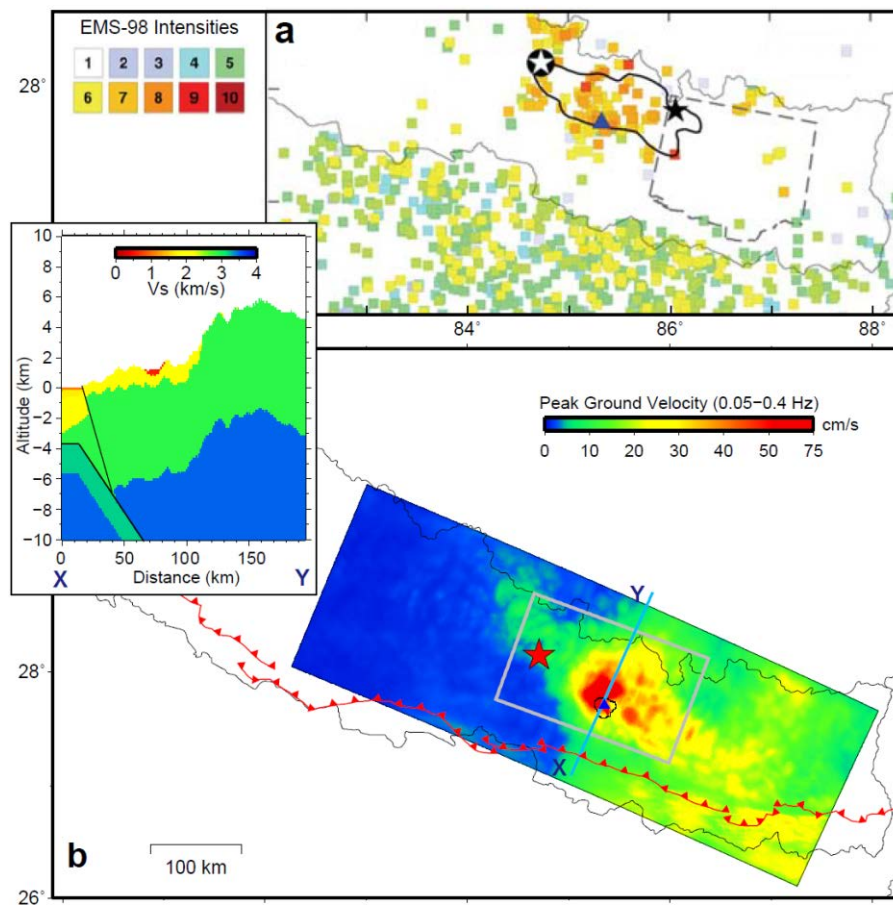
Figure 4. Distributions of observed intensities and simulated ground velocities. The Intensity distribution in **a** was obtained by Martin et al. (2015; © Seismological Society of America).

To confirm the above, we conducted ground motion simulations using the finite-element method (FEM) with a voxel mesh. A preliminary model of three-dimensional (3-D) velocity structure had been constructed for this simulation, based on a geological profile in central Nepal, global relief data, a global model of Earth's crust, and a geological model of the Kathmandu Valley (inset of Fig. 4b). Simulated ground motions were filtered with a passband of 0.05 to 0.4 Hz, which covers significant frequency contents of observed velocity seismograms, but the buildings that collapsed and caused fatalities would likely be most sensitive to higher frequencies.

It was found that the resultant distribution of peak ground velocities in Fig. 4b simulates the intensity distribution (Fig. 4a) augmented by the fatality rate distribution fairly well, if we refer to the relationship of intensities and peak ground velocities.

The fatality rate was used only to compensate for the missing part of the intensity distribution. In particular, large ground velocities are spread far to the east in a similar manner to the augmented intensity distribution. However, moderate ground velocities also extend south-east to the Indo-Gangetic Plain beyond the MFT. This is, in part, consistent with the observation that at least 78 people were killed and 560 were injured in India, although the intensities in the southernmost part of Nepal beyond the MFT were limited, as shown in Fig. 4a.

REFERENCES

Koketsu, K., Miyake, H., Guo, Y., Kobayashi, H., Masuda, T., Davuluri, S., Bhattarai, M., Adhikari, L. B. and Sapkota, S. N. (2016) Widespread ground motion distribution caused by rupture directivity during the 2015 Gorkha, Nepal earthquake. Scientific Reports, Vol 6, 28536; doi:10.1038/srep28536.

Martin, S. S., Hough, S. E. and Hung, C. (2015) Ground motions from the 2015 M_{w} 7.8 Gorkha, Nepal, earthquake constrained by a detailed assessment of macroseismic data, Seismol. Res. Lett., Vol 86, pp 1524-1532.